

Review of Analysis and Modeling Techniques for Incompressible, Turbulent Bluff-Body Wakes

Logan D. Halstrom* and Federico Zabaleta†
University of California, Davis, California, 95616

abstract here *LH&FZ*

Nomenclature

LH&FZ

ρ = density, kg/m^3

Subscripts

(∞) = freestream quantity

Acronyms

CFD = Computational Fluid Dynamics

I. Introduction

INTRO sentence to paper should have this fancy capitalization.

I. • Driving Physical Phenomena *FZ*

- differences from potential flow
- blunt/bluff body definition, differences from streamlined body flow
- massively separated flow
- base pressure
- wake

I. • Real World Applications *LH*

- parachute
- reentry capsule
- vehicles
- buildings
- show similarity between cylinder/sphere wake and more complex bluff body

*Graduate Student, Mechanical And Aerospace Engineering Department, One Shields Avenue

†Graduate Student, Civil and Environmental Engineering Department, One Shields Avenue

Big whorls have little whorls, which feed on their velocity, and little whorls have lesser whorls, and so on to viscosity (in the molecular sense). Richardson (1922) [1]

II. Experimental Methods And Results

FZ

- Historical Study
- Experimental techniques
 - ballistic range?
- Applications
 - Simple cases: cylinder/sphere
 - * Drag vs Re?
 - * Wake velocity profiles?
 - * Wake structure?
 - Sharp vs bluff: sphere vs cube
 - Complex cases: capsule/building

III. Computational Methods and Results

LH

- Historical Study
- Computational techniques
- Applications
 - Simple cases: cylinder/sphere
 - Sharp vs bluff: sphere vs cube
 - Complex cases: capsule/building

A. Turbulence Modeling Aspects

LH

- Brief turbulence model description
 - RANS vs URANS
 - DNS
 - LES (uses DNS) and DES (=Hybrid RANS/LES)
- Compare turbulence model performance for sphere/cylinder
 - DES > URANS > RANS

- DES = functional LES
- SAS vs DES?
- DNS: limited Re
- Shortcomings of each model (and how to address them)
 - URANS
 - DES: only good at sharp separation
 - * “An order of accuracy has not even been proposed for a simulation using both modes within DES”
 - Spalart about hybrid method
 - * grid induced separation (maybe not an issue for bluff bodies)
 - * DES can default to RANS if grid adaptation misses a shear layer
- Advanced geometries
 - f-15
 - car
 - building
 - capsule
 - chute, landing gear, helicopter, wind turbine

LIST ALL FIGURES HEAR, REORDER AND DESCRIBE LATER

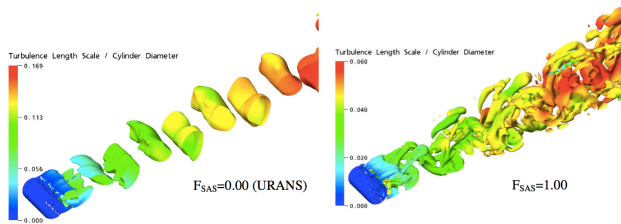


Fig. 1 SAS vs URANS cylinder [2]

Figure 5: Resolved structures for cylinder in crossflow using different constants FSAS

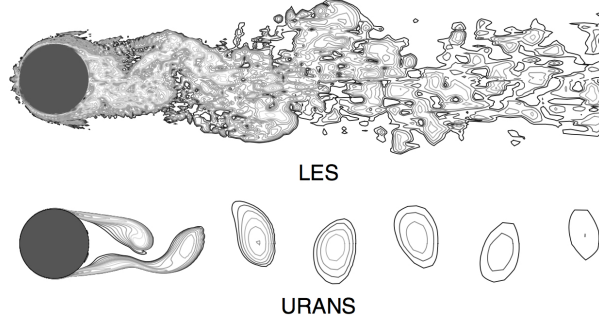


Fig. 2 cylinder les vs urans instantaneous [3]

Instantaneous vorticity magnitude at a given spanwise cut for flow over a circular cylinder at $ReD = 106.25$ contour levels from $xD=U_1/4$ to $xD=U_1/4 575$ (exponential distribution) are plotted.

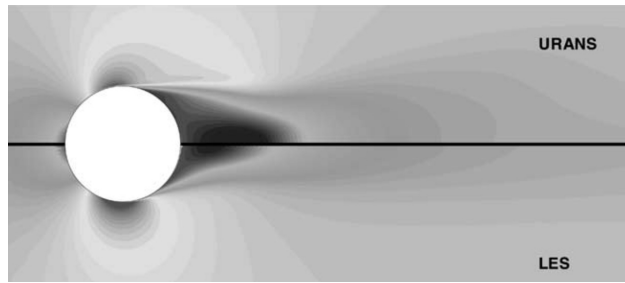


Fig. 3 cylinder les vs urans averaged [3]

Fig. 5. Mean streamwise velocity distribution predicted by LES and URANS. 45 contour levels from $U=U_1/4 0:2$ to $U=U_1/4 1:7$ are plotted.

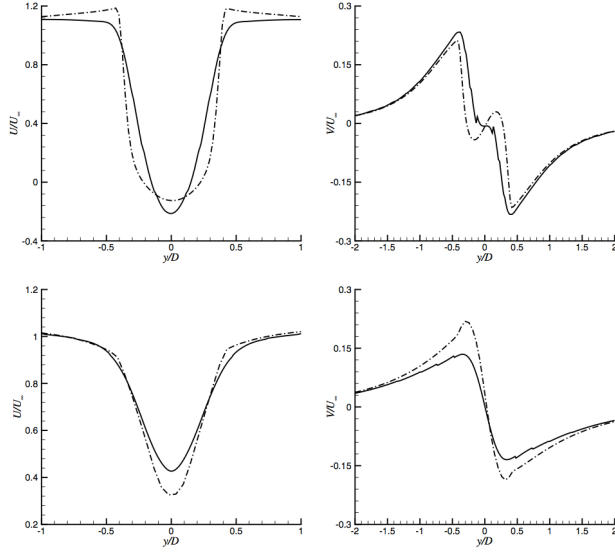


Fig. 4 cylinder les vs urans velocity profiles [3]

Fig. 6. Mean streamwise and vertical velocities at $x=D 1/4 0.75$ (upper figures) and $x=D 1/4 1.50$ (lower figures):
 (—) LES; (--) URANS

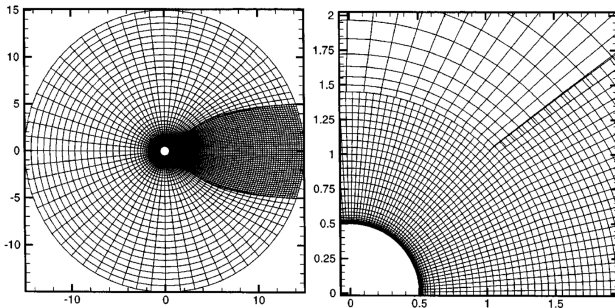


Fig. 5 cylinder les vs rans grid [4]

Figure1. Medium computational grid, CaseTS2. Innerblock 150×36 , wakeblock 74×36 , outer block 59×30 . The three blocks meet near $x = 1.06$, $y = 1.03$. Grid for spalart cylinders.

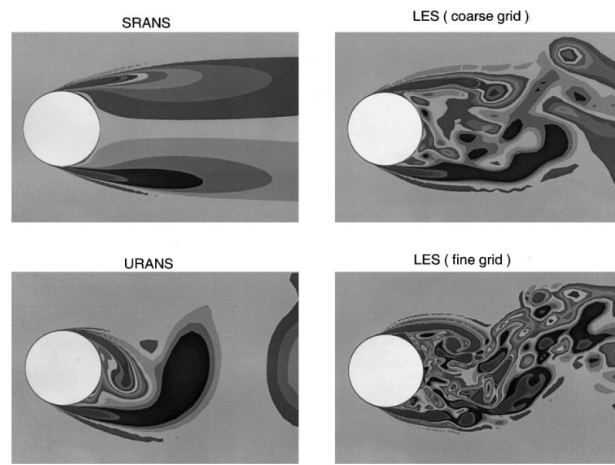
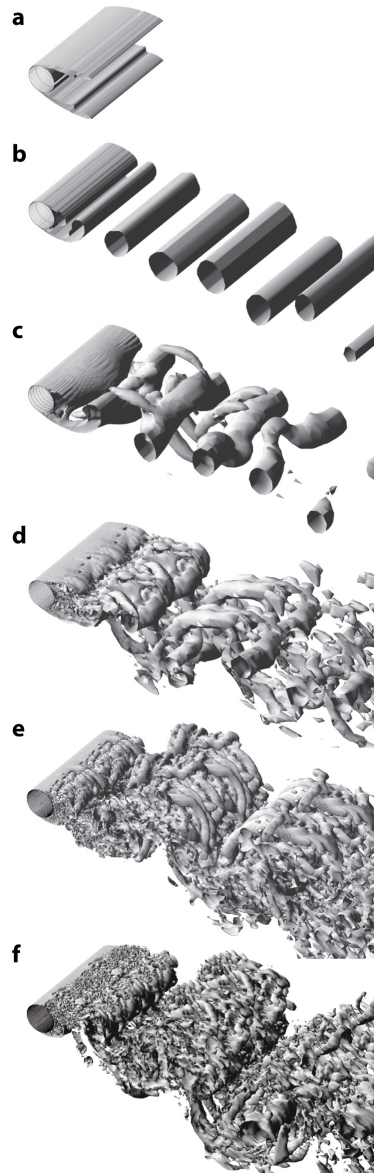


Fig. 6 cylinder les vs rans [5]

grid for LES shown above (actual simulations were DES)



 Spalart PR. 2009.
Annu. Rev. Fluid Mech. 41:181–202

Fig. 7 cylinder simulation with RANS, 2DURANS, 3DURANS, SSTDES, SADES [6]

Vorticity isosurfaces by a circular cylinder: $ReD = 5 \times 10^4$, laminar separation. Experimental drag coefficient $C_d = 1.15\text{--}1.25$. (a) Shear-stress transport (SST) turbulence model steady Reynolds-averaged Navier-Stokes (RANS), $C_d = 0.78$; (b) SST 2D unsteady RANS, $C_d = 1.73$; (c) SST 3D unsteady RANS, $C_d = 1.24$; (d) Spalart-Allmaras (SA) detached-eddy simulation (DES), coarse grid, $C_d = 1.16$; (e) SA DES, fine grid, $C_d = 1.26$; (f) SST DES, fine grid, $C_d = 1.28$. Figure courtesy of A. Travin

illustrates the response of DES to grid refinement in its LES region.

DES solutions with different base RANS models are not sensitive to model choice in the LES region (as opposed to the RANS region, particularly if separation occurs).

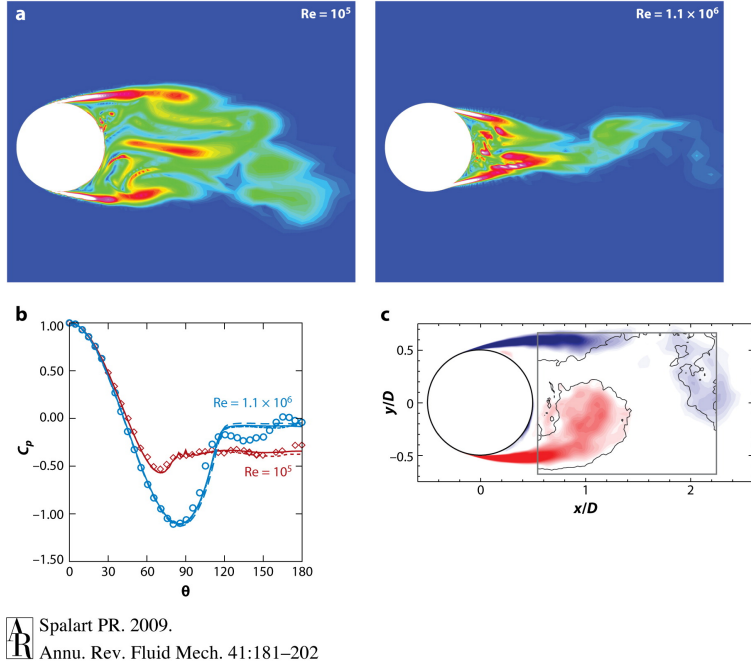


Fig. 8 DES validation from [6]. Sphere transition and drag crisis from [7]. Vorticity validation from [8]

Simple bluff bodies. (a) Flow visualizations and (b) pressure distributions for a sphere. $Re = 10^5$ and 1.1×10^6 . Open circles and diamonds denote experiments, whereas the dotted and dashed lines denote detached-eddy simulation (DES) on two grids. Panels a and b courtesy of K. Squires. (c) Phase-averaged vorticity contours for a cylinder. Color gradations denote DES conducted by Mockett et al. (2008), and the solid line denotes experiments by the same authors.

NOTE: DES could be used to emulate the dimples on a golf ball by setting the boundary layer separation point, but true simulation of flow in golf ball dimples requires DNS due to the range of scales

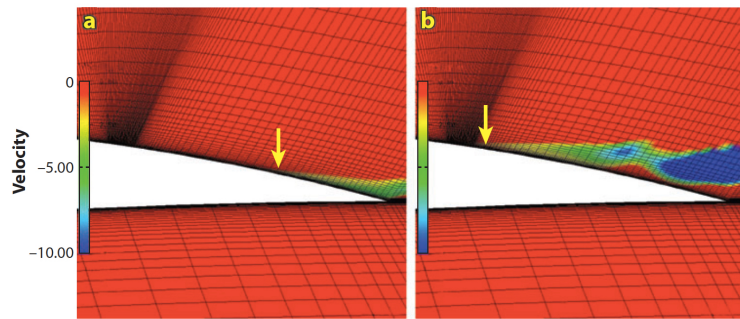


Fig. 9 Example of DES grid induced separation from [6], source: [9]

Vorticity contours over an airfoil: (a) Reynolds-averaged Navier-Stokes and (b) detached-eddy simulation. Arrows indicate separation. Figure taken from Menter & Kuntz 2002.

Potential con of using DES. EXPLAIN HOW GRID INDUCED SEPARATION WORKS.

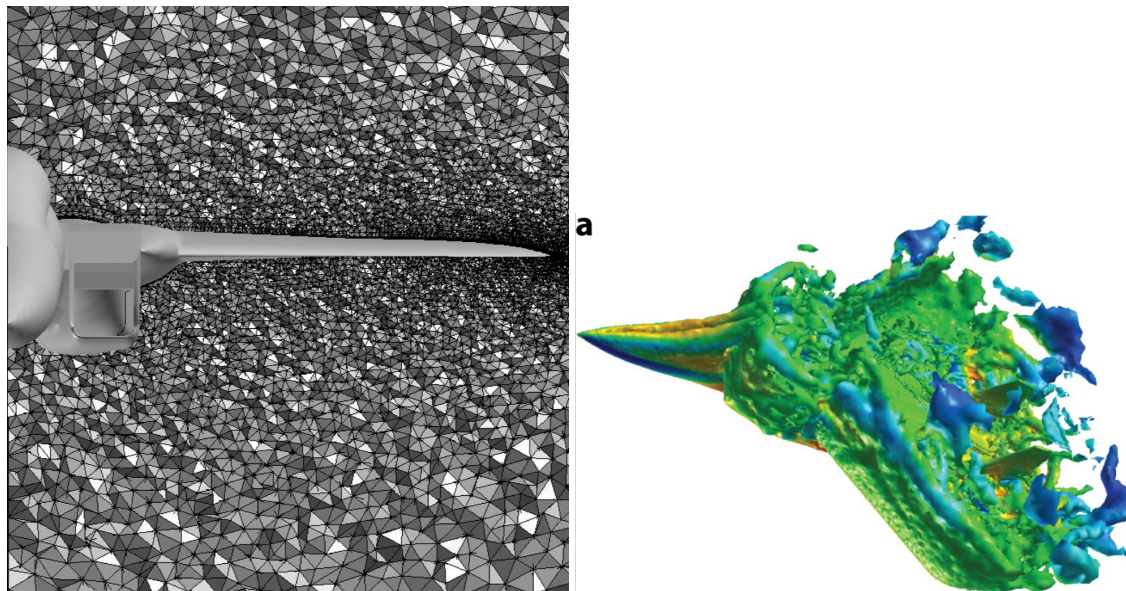


Fig. 10 F-15 DES grid (left) [10] vorticity isocontours (right) [6]

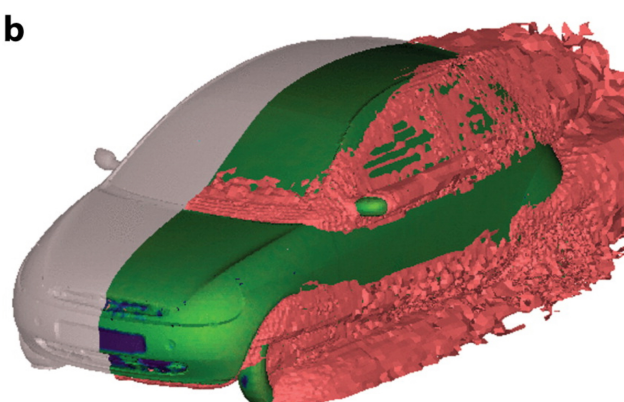


Fig. 11 car DES isocontours [11]

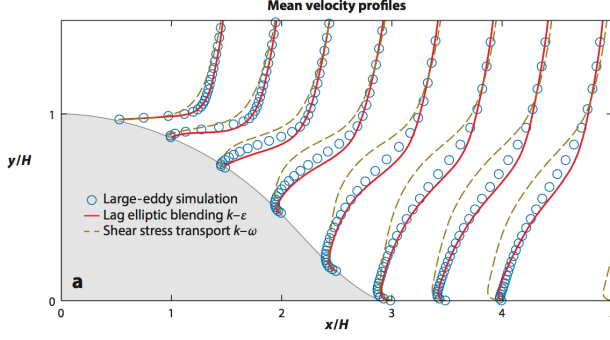


Fig. 12 curve backstep velocity profile les vs rans [12]

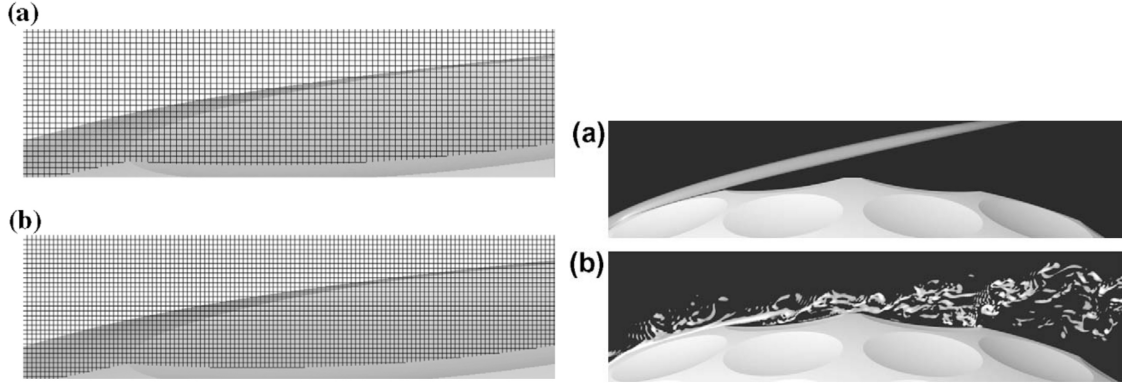


Fig. 13 DNS non-rotating golf ball with dimples grid (left) vorticity (right) [13]

Example grid resolution in a dimple near 84° (measured from the stagnation point at the front of the golf ball). (a) $\text{Re} = 2.5 \cdot 10^4$; (b) $\text{Re} = 1.1 \cdot 10^5$.

Contours of azimuthal vorticity. (a) $\text{Re} = 2.5 \cdot 10^4$; (b) $\text{Re} = 1.1 \cdot 10^5$

NOTE: Recall sphere example from Spalart review and say that this is the analogous DNS experiment to his DES

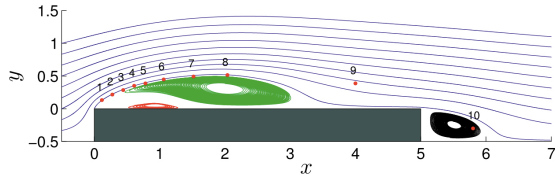


Fig. 14 DNS square cylinder vortex locations $\text{Re}=3000$ [14]

Fig. 4. Streamlines of the mean velocity field (U, V) (x, y) The green lines show the primary vortex, the red lines mark the secondary vortex and the black lines denote the wake vortex. The red dots denote the locations of the probes used for the computation of time spectra in section x5. (For interpretation of the references to color in this figure legend,

the reader is referred to the Web version of this article.)

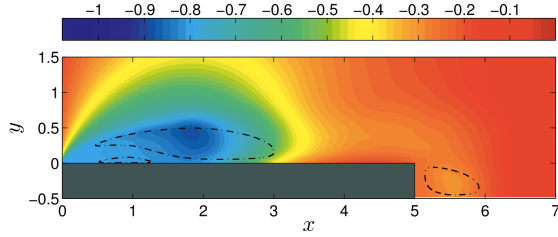


Fig. 15 DNS square cylinder mean pressure distribution Re=3000 [14]

Fig. 5. Isocontours of the mean pressure field $P(x,y)$. The dashed lines report the location of the primary vortex, secondary vortex and wake vortex.

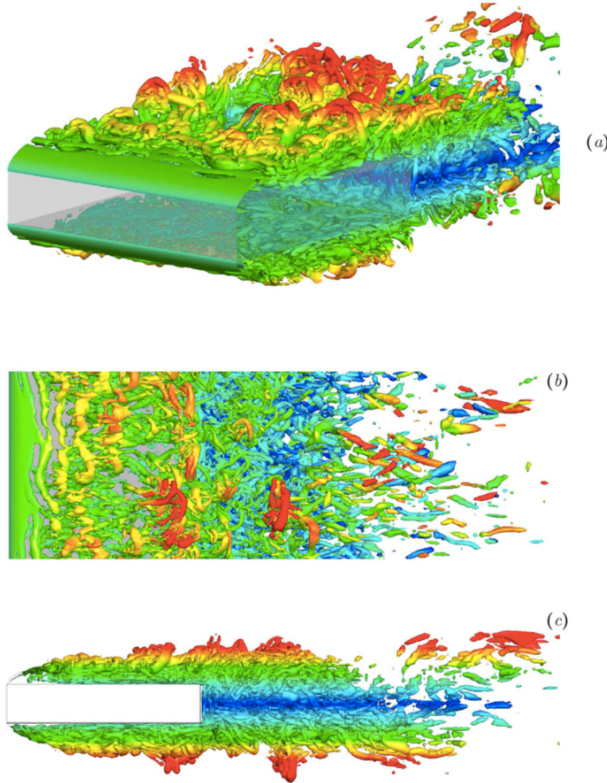


Fig. 16 DNS square cylinder vorticity contours Re=3000 [14]

Fig. 10. Instantaneous isosurfaces of $\lambda_2 = -2$ colored with y . Perspective, top and lateral views in (a), (b) and (c) plots, respectively.

IV. Current State of Bluff-Body Turbulence Analysis

- Current State of Knowledge

- Remaining Challenges

A. Experimental Methods

FZ

B. Computational Methods

LH

V. Conclusions

LH&FZ

Acknowledgments

LH&FZ

Example citations

[15]

References

- [1] Richardson, L. F., *Weather Prediction by Numerical Process*, Cambridge University Press, Cambridge, UK, 1922.
- [2] Menter, F., and Egorov, Y., “A Scale Adaptive Simulation Model using Two-Equation Models,” *43rd AIAA Aerospace Sciences Meeting and Exhibit, Aerospace Sciences Meetings*, Reno, NV, January 2005.
- [3] Catalano, P., Wang, M., Iaccarino, G., and Moin, P., “Numerical simulation of the flow around a circular cylinder at high Reynolds numbers,” *International Journal of Heat and Fluid Flow*, Vol. 24, No. 4, 2003, pp. 463 – 469. doi:[https://doi.org/10.1016/S0142-727X\(03\)00061-4](https://doi.org/10.1016/S0142-727X(03)00061-4), URL <http://www.sciencedirect.com/science/article/pii/S0142727X03000614>, selected Papers from the Fifth International Conference on Engineering Turbulence Modelling and Measurements.
- [4] Travin, A., Shur, M., Strelets, M., and Spalart, P., “Detached-Eddy Simulations Past a Circular Cylinder,” *Flow, Turbulence and Combustion*, Vol. 63, No. 1, 2000, pp. 293–313. doi:[10.1023/A:1009901401183](https://doi.org/10.1023/A:1009901401183), URL <https://doi.org/10.1023/A:1009901401183>.
- [5] Spalart, P., “Strategies for turbulence modelling and simulations,” *International Journal of Heat and Fluid Flow*, Vol. 21, No. 3, 2000, pp. 252 – 263. doi:[https://doi.org/10.1016/S0142-727X\(00\)0007-2](https://doi.org/10.1016/S0142-727X(00)0007-2), URL <http://www.sciencedirect.com/science/article/pii/S0142727X00000072>.
- [6] Spalart, P. R., “Detached-Eddy Simulation,” *Annual Review of Fluid Mechanics*, Vol. 41, No. 1, 2009, pp. 181–202. doi:[10.1146/annurev.fluid.010908.165130](https://doi.org/10.1146/annurev.fluid.010908.165130), URL <https://doi.org/10.1146/annurev.fluid.010908.165130>.

- [7] Squires, K. D., “Detached-Eddy Simulation: Current Status and Perspectives,” *Direct and Large-Eddy Simulation V*, edited by R. Friedrich, B. J. Geurts, and O. Métais, Springer Netherlands, Dordrecht, 2004, pp. 465–480.
- [8] Mockett, C., Greschner, B., Knacke, T., Perrin, R., Yan, J., and Thiele, F., “Demonstration of Improved DES Methods for Generic and Industrial Applications,” *Advances in Hybrid RANS-LES Modelling*, edited by S.-H. Peng and W. Haase, Springer Berlin Heidelberg, Berlin, Heidelberg, 2008, pp. 222–231.
- [9] Menter, F. R., and Kuntz, M., “Adaptation of Eddy-Viscosity Turbulence Models to Unsteady Separated Flow Behind Vehicles,” *The Aerodynamics of Heavy Vehicles: Trucks, Buses, and Trains*, edited by R. McCallen, F. Browand, and J. Ross, Springer Berlin Heidelberg, Berlin, Heidelberg, 2004, pp. 339–352.
- [10] Forsythe, J. R., Squires, K. D., Wurtzler, K. E., and Spalart, P. R., “Detached-Eddy Simulation of the F-15E at High Alpha,” *Journal of Aircraft*, Vol. 41, No. 9, 2004, pp. 193–200.
- [11] Mendonça, F., Allen, R., de Charentenay, J., and Lewis, M., “Towards Understanding LES and DES for Industrial Aeroacoustic Predictions,” *International workshop on ‘LES for Acoustics’*, DLR Göttingen, Germany, October 2002.
- [12] Durbin, P. A., “Some Recent Developments in Turbulence Closure Modeling,” *Annual Review of Fluid Mechanics*, Vol. 50, No. 1, 2018, pp. 77–103. doi:10.1146/annurev-fluid-122316-045020.
- [13] Smith, C., Berathis, N., Balaras, E., Squires, K., and Tsunoda, M., “Numerical investigation of the flow over a golf ball in the subcritical and supercritical regimes,” *International Journal of Heat and Fluid Flow*, Vol. 31, No. 3, 2010, pp. 262 – 273. doi: <https://doi.org/10.1016/j.ijheatfluidflow.2010.01.002>, URL <http://www.sciencedirect.com/science/article/pii/S0142727X10000147>, sixth International Symposium on Turbulence and Shear Flow Phenomena.
- [14] Cimarelli, A., Leonforte, A., and Angeli, D., “Direct numerical simulation of the flow around a rectangular cylinder at a moderately high Reynolds number,” *Journal of Wind Engineering and Industrial Aerodynamics*, Vol. 174, 2018, pp. 39 – 49. doi:<https://doi.org/10.1016/j.jweia.2017.12.020>, URL <http://www.sciencedirect.com/science/article/pii/S0167610517304622>.
- [15] Nakamura, Y., “Bluff-body aerodynamics and turbulence,” *Journal of Wind Engineering and Industrial Aerodynamics*, Vol. 49, No. 1, 1993, pp. 65 – 78. doi:[https://doi.org/10.1016/0167-6105\(93\)90006-A](https://doi.org/10.1016/0167-6105(93)90006-A), URL <http://www.sciencedirect.com/science/article/pii/016761059390006A>.